



Building a new space weather facility at the National Observatory of Athens

Ioannis Kontogiannis^{*}, Anna Belehaki, Georgia Tsiropoula, Ioanna Tsagouri,
Anastasios Anastasiadis, Athanasios Papaioannou

Institute for Astronomy, Astrophysics, Space Applications and Remote Sensing, National Observatory of Athens, GR-15236 Penteli, Greece

Received 6 February 2015; received in revised form 11 September 2015; accepted 21 October 2015

Available online 30 October 2015

Abstract

The PROTEAS project has been initiated at the Institute of Astronomy, Astrophysics, Space Applications and Remote Sensing (IAASARS) of the National Observatory of Athens (NOA). One of its main objectives is to provide observations, processed data and space weather nowcasting and forecasting products, designed to support the space weather research community and operators of commercial and industrial systems. The space weather products to be released by this facility, will be the result of the exploitation of ground-based, as well as space-borne observations and of model results and tools already available or under development by IAASARS researchers. The objective will be achieved through: (a) the operation of a small full-disk solar telescope to conduct regular observations of the Sun in the H-alpha line; (b) the construction of a database with near real-time solar observations which will be available to the community through a web-based facility (HELIOSEVER); (c) the development of a tool for forecasting Solar Energetic Particle (SEP) events in relation to observed solar eruptive events; (d) the upgrade of the Athens Digisonde with digital transceivers and the capability of operating in bi-static link mode and (e) the sustainable operation of the European Digital Upper Atmosphere Server (DIAS) upgraded with additional data sets integrated in an interface with the HELIOSEVER and with improved models for the real-time quantification of the effects of solar eruptive events in the ionosphere.

© 2015 COSPAR. Published by Elsevier Ltd. All rights reserved.

Keywords: Solar activity; Space weather; Monitoring; Ionosphere; Ionospheric disturbances; Solar Energetic Particles

1. Introduction

The near-Earth space environment is subject to the abrupt events of solar activity, the most dramatic of which are solar flares and Coronal Mass Ejections (CMEs). Flares are sudden and intense brightenings that occur in Active Regions (ARs). They are visible across the entire electromagnetic spectrum, quite prominent in UV, X-rays

and optical lines, like H α (Fletcher et al., 2011). Often associated with flares are CMEs, although no causal relationship has been established between them. CMEs reach very high velocities (Webb and Howard, 2012) disrupting the constant flow of solar wind, and affecting the near-Earth space environment in numerous ways. Both flares and CMEs are sources of Solar Energetic Particles (SEPs) produced as a result of the diffusive processes on the solar atmosphere and/or acceleration on the interplanetary shock fronts of Interplanetary CMEs (ICMEs).

Solar flares eject enormous amounts of energy into outer space in a very short time ranging from a few minutes to a few hours that can affect the near-Earth space environment in numerous ways. Energetic particles (ions) of 10 keV to

^{*} Corresponding author.

E-mail addresses: jkonto@noa.gr (I. Kontogiannis), belehaki@noa.gr (A. Belehaki), georgia@noa.gr (G. Tsiropoula), tsagouri@noa.gr (I. Tsagouri), anastasi@noa.gr (A. Anastasiadis), atpapaio@noa.gr (A. Papaioannou).

GeV energies are accelerated at the flare site, while electrons with energies up to several MeV are also created (Anastasiadis, 2002). Fast ICMEs that may be associated with solar flares have upstream shocks which accelerate ions to ~ 10 keV to ~ 10 MeV. In the case of solar flares the energetic particles reach the Earth's ionosphere shortly after the flare photons, while in the case of CMEs, energetic particles are continuously produced and bombard the Earth's upper atmosphere following the formation of the ICME at a distance of ~ 3 – $10 R_S$ from the Sun and its propagation from the formation site to 1 AU and beyond (from about 1 hr up to 4 days) (Tsurutani et al., 2009). When the ICME reaches the magnetosphere about 1 to 4 days later, shock compression of the magnetosphere energizes preexisting 10–100 keV magnetospheric electrons and ions, causing precipitation into the dayside auroral zone ionosphere. Shock compression can also trigger supersubstorms in the magnetotail with concomitant energetic particle precipitation into the nightside auroral zones (Tsurutani et al., 2009). It should be further noted that the origin, acceleration and propagation of energetic particles is still unresolved and that apart from the dominant accelerators (i.e. solar flares and CME-driven shocks), the interplay of two variable factors, e.g. shock geometry and seed population, provide a framework for understanding the variability at high energies in large SEP events (Tylka et al., 2005).

In the Earth's ionosphere, geoeffective CMEs can lead to positive and negative ionospheric storms, depending on the local time of the observing location in the ionosphere and the geomagnetic latitude. According to the Prölss phenomenological scenario (Prölss, 1993; Prölss, 1995), solar wind energy input injection to the polar upper atmosphere, activates the meridional winds system, launching a so-called traveling atmospheric disturbance (TAD) that causes at middle latitudes daytime positive storm effects (enhancement of ionization) of short duration by an uplifting of the F2 layer. On the other hand, the dissipation of solar wind energy input changes the neutral gas composition, generating a permanent composition disturbance zone at polar latitudes that causes negative storm effects (depletion of ionization). During disturbed conditions this zone expands toward middle latitudes in the early morning sector due to winds of moderate magnitude, designated as midnight surge (Szuszczewicz et al., 1998; Tsagouri et al., 2000; Belehaki and Tsagouri, 2002).

Even in the absence of CMEs, solar flares have direct and immediate consequences on the ionosphere. The enhanced EUV and X-ray emissions create, at a very short time scale of a few minutes, extra ionization of the neutral components in the Earth's upper atmosphere and, hence, immediate increases in the electron density over a wide altitude range from the ionospheric D region up to the F region (Thomson et al., 2004; Liu et al., 2007). This consequently leads to various Sudden Ionospheric Disturbances (SIDs) that have important effects on radio communications and navigations over the entire radio spectrum (Liu et al., 2004). In particular shortwave fadeouts (SWF),

abnormally strong absorptions in the ionosphere, occur as the immediate result of solar flare eruptions, leading to fadeouts in high-frequency radio propagation. The SWF is attributed to the X-rays emitted from the flare. The EUV radiation also contributes to other types of SIDs. In fact, different effects are observed during the various phases of a solar flare: the EUV radiation and the hardest X-rays tend to be enhanced early in the flare, whereas the softer X-rays last longer and correspond more closely with the optical flare. Though the effects are mostly registered in the D region, E and F region effects can also be detected. The D-region effect is due to the hardest X-rays. The electron content, governed mainly by the F region, is increased by a few per cent and it is due to the EUV radiation. Another effect of the EUV radiation is the reduction of the reflection height in E and F layers.

To recapitulate, the chain of events and interconnections described so far demonstrate the dynamic nature of the geospace environment. The time scales characteristic of the evolution of these phenomena vary from a few minutes up to days. Due to the rapidly growing interest and dependence of human activities on space technologies this gamut of time scales complicates prediction and modeling of the effects relevant to space weather. To successfully forecast space weather, first of all, a better understanding of the physical processes involved is needed. Apart from that and in order to minimize its impacts, a robust capability of monitoring the Sun, the interplanetary medium and the ionosphere with ground- and space-based observing instruments is needed to support operational space weather forecasting. Observations and extracted parameters from these observing systems can be used as input to prediction models to produce nowcasts and short- or long-term forecasts.

To facilitate progress in the field, the scientific community has been very active in putting together archives with diverse data from solar and space observations and measurements, such as the Heliophysics Event Knowledgebase (HEK¹), the Solar Influences Data Analysis Center (SIDC²), the European Near-Earth Space Data Infrastructure for e-Science (ESPAS³), the Heliophysics Integrated Observatory (HELIO⁴), etc. In parallel, a number of targeted services has been established aiming at the specification of the space weather effects in the Earth's magnetosphere and ionosphere to meet the users' requirements. Such services have been integrated into the Space Weather Prediction Center (SWPC⁵) of the National Oceanic and Atmospheric Administration (NOAA) in the USA, and the Space Weather Service Network developed under the Space Situational Awareness (SSA⁶) programme of

¹ <http://www.lmsal.com/hek/>.

² <http://sidc.oma.be/>.

³ <http://www.espas-fp7.eu>.

⁴ <http://www.helio-vo.eu/>.

⁵ <http://www.swpc.noaa.gov/>.

⁶ <http://swe.ssa.esa.int/>.

the European Space Agency (ESA) in Europe. Considerable progress in the field has also been achieved through a significant number of national and international initiatives that were launched in the last decade to cover special needs. Relevant European investments include, to name some examples: the European Digital Upper Atmosphere Server (DIAS⁷) for ionospheric products and services relevant to HF communication users for the European region; the Space Weather Application Center – Ionosphere (SWACI⁸; Jakowski et al., 2009, 2011) in support of ionospheric and trans-ionospheric propagation purposes; the COronal Mass Ejections and Solar Energetic Particles (COMESSEP⁹) project that developed tools for forecasting geomagnetic storms and solar energetic particle radiation storms and the Advanced Forecast For Ensuring Communications Through Space project (AFFECTS¹⁰), which provides real time monitoring of the geospace and issues reports, forecasts and alerts on solar wind and space weather to protect communication systems. In some projects, monitoring the solar activity and space weather are also accompanied by ground based observations, since observations, classification and prediction of solar active regions and flares is relatively easy to implement with ground-based telescopes (Gallager et al., 2002; Pötzi et al., 2015). This is the case for e.g. the SolarMonitor¹¹ and the Bureau of Meteorology in Australia (the former Ionospheric Prediction Service, IPS¹²).

In this frame, a new project called PROTEAS (an acronym in Greek, for Advanced Space Applications for the Exploration of the Universe, Space and Earth) has been initiated recently at the IAASARS/NOA. One of its objectives is to exploit the existing ionospheric facilities and services along with prediction models and tools, already available or under development and implementation at the Institute, towards the establishment of an integrated space weather facility that will be based on solar and ionospheric observations, obtained by the team, and space measurements, which are publicly available. The new facility aims to strengthen current space weather prediction capabilities of NOA both in national and regional scale and to provide the research community with new data and tools that are complimentary to existing efforts. It will also help advances towards the efficient specification of space weather effects in the near-Earth space environment down to the height of the bottomside ionosphere for operational and research applications.

To reach its objectives, the project activities are developed along two lines of action: monitoring and forecasting/alerting. In this paper, these particular objectives of the PROTEAS project are described. Current available

observational facilities and techniques are presented in Section 2. They include the observation of the solar atmosphere using an H α solar telescope and real-time measurements of the ionosphere using the Athens Digisonde. The ionospheric predictions are based on the DIAS (described in Section 2.3) relevant services of nowcasting and forecasting. Section 3 presents the development of new monitoring services and space weather prediction tools. Specifically, a forecasting tool for SEPs is being developed and will be integrated to the provided services (Section 3.2). The final products together with the obtained H α observations will be available to the community in near real-time through a web-based server, the HELIOSERVER (Section 3.3). The potential of this endeavor is demonstrated by two examples in Section 4. The paper ends with a conclusion and discussion concerning how the user, as well as the scientific community, will benefit from the provided products.

2. Existing observational facilities and services

2.1. Solar telescope for H α imaging

For chromospheric imaging, an H α solar dedicated telescope was selected. Manufactured by *Lunt Solar Systems*, it is a 100 mm refractor, with 800 mm focal length also equipped with a 1800 mm blocking filter. It has an in-built H α etalon with a bandpass lower than 0.75 Å, which may be further reduced to lower than 0.5 Å, when doublestacked with a second H α etalon. A pressure tuner enables tuning along H α for the imaging of Doppler-shifted features. The solar telescope is placed inside a dome on the premises of the *National Observatory of Athens*, at Penteli, near Athens, Greece.

Imaging is performed with a *DMK51AU02* CCD camera (by *The Imaging Source*), equipped with a *Sony ICX274AL* sensor, with 1600 × 1200 pixel resolution and 4.4 × 4.4 μm pixel dimension. The setup provides near-full-disk images of the Sun with an estimated 1.6'' resolution and 1.27'' per pixel in 1 × 1 binning. Acquired images will feed a real-time processing pipeline at the working station to produce high quality, full disk images along with close-ups of ARs of interest. The latter will be implemented via an appropriately modified optical assembly (using Barlow lenses and focal reducers) to achieve smaller field of view and spatial scale.

2.2. The Athens Digisonde

The National Observatory of Athens operates a Digitally Integrating Goniometric Ionosonde (DIGISONDE) since 2000, making available vertical ionograms and drift measurements in real time, through <http://www.iono.noa.gr>. For the needs of this project, the Athens Digisonde has been upgraded to a DPS4D advanced Digital ionospheric station. The station is equipped with digital transceivers having capability for superior accuracy, precision, and

⁷ <http://dias.space.noa.gr>.

⁸ <http://swaciweb.dlr.de/>.

⁹ <http://comesep.aeronomy.be/>.

¹⁰ <http://www.affects-fp7.eu/>.

¹¹ www.solarmonitor.org.

¹² <http://www.ips.gov.au/>.

resolution of amplitude and phase measurements, precision echolocation for skymaps, precision ranging for ionogram traces and a new Radio Frequency Interference Mitigation technique leading to a 40 dB signal to noise ratio improvement. Finally the new Athens Digisonde is capable of performing in automatic bi-static sounding mode (Fig. 1). Exploiting the capability of fast measurements (2 s ionograms) offered by the new receiver, the Athens Digisonde is able to detect the effects of abrupt solar activity events in the mid-latitude ionosphere in different time scales. The immediate effects due to the enhanced emission can be detected as enhancement of the Total Electron Content (TEC) and reduction of hmE and hmF2 parameters (peak height of the E- and F2- layers respectively). Being at middle latitudes, the Athens Digisonde can detect both positive and negative ionospheric storms triggered by ICMEs and the proposed Space Weather facility will exploit its recordings for nowcasting and forecasting purposes of ICME effects in the ionosphere.

2.3. The European Digital Upper Atmosphere Server (DIAS)

DIAS operates since 2007 and provides products and services that characterize ionospheric conditions over Europe. After several upgrades, today DIAS releases a large number of products for the specification, forecasting and prediction of the ionosphere and the plasmasphere useful for both scientific and operational applications.

DIAS is a distributed information server, capable of supporting the acquisition, evaluation and processing of a number of data sets streaming in real time from observing platforms (Belehaki et al., 2005, 2006, 2007). Processed data are digested into a java library of semi-empirical models that calculate products for nowcasting and forecasting conditions in the bottomside and topside ionosphere and

in the plasmasphere. DIAS operation is compliant with the EU open access policy for scientific data and it is based on the analysis of data streaming from ionosondes operated in Athens, Rome, Ebre, Arenosillo, Chilton, Juliusruh, Pruhonice, Moscow, Tromso and Sodankyla, assisted by supporting data sets, such as geomagnetic and solar indices and solar wind parameters from the NASA Advanced Composition Explorer (ACE) spacecraft. The semi-empirical models included in the DIAS java library are renewed often in order to follow the latest state of the art. Below we present shortly the main prediction models included in the current version of the DIAS java library:

- The Simplified Ionospheric Regional Model (SIRM), which is a long-term prediction model that provides the key ionospheric characteristics, for the European region (Zolesi et al., 1993). SIRM results are updated in real-time with ionospheric observations streaming from the DIAS ionosondes to adjust the climatological estimates to nowcasting conditions, and to produce now-casting maps over Europe (Zolesi et al., 2004).
- The Solar Wind driven autoregression model for Ionospheric short-term Forecast (SWIF) was developed by Tsagouri and Belehaki (2008), Tsagouri et al. (2009) and validated by Tsagouri (2011). SWIF combines near real-time and past ionospheric observations with solar wind parameters at the L1 point, provided by NASA/ACE spacecraft through the cooperation of a model that forecasts the non-storm ionosphere. The model predictions are triggered by an alert signal for upcoming ionospheric disturbances obtained from the real-time analysis of interplanetary magnetic field (IMF) data, from the ACE spacecraft. The alert algorithm is based on specific criteria that have been derived applying superposed epoch analysis on the magnetic field data from ACE for intense storm events occurring during

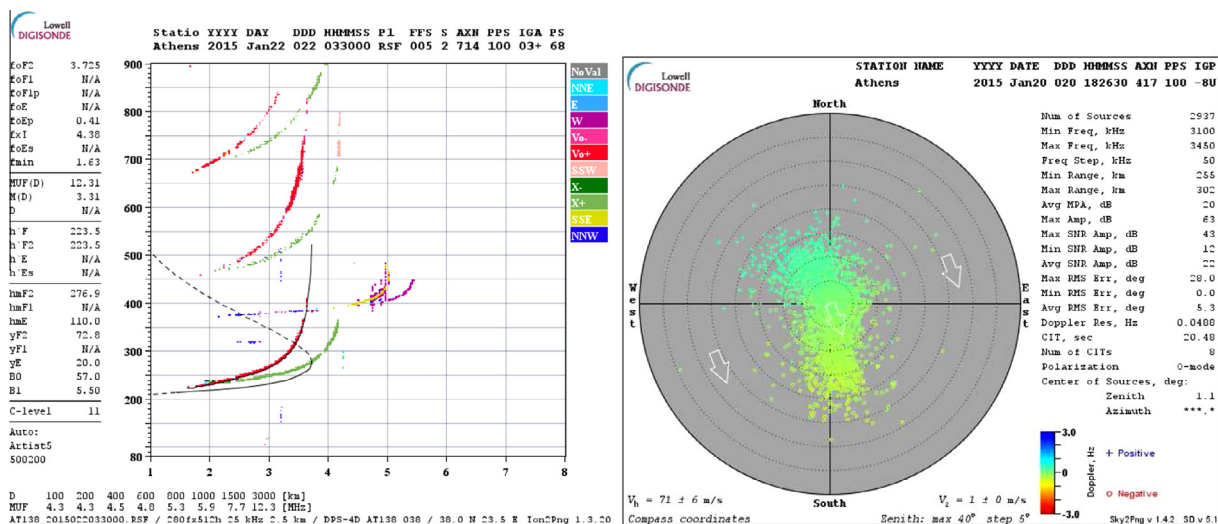


Fig. 1. Left: Doppler ionogram from the Athens Digisonde DPS4D in bi-static link with similar DPS4D operated in San Vito (Central Italy). Right: skyplot from the Athens Digisonde measuring drifting ionospheric plasma in the F-layer height, moving to the south.

solar cycle 23. These events were mainly driven by CME-associated flows at L1 (Tsagouri and Belehaki, 2015).

- The Topside Sounders Model-Assisted by Digisondes (TaD), is a topside reconstruction model for the Electron Density Profile (EDP) up to the GNSS heights. The current TaD routine includes also a mapping procedure in order to transform single point EDP to 2D TEC maps. The TaD model is a topside profiler based on empirical equations derived from topside sounding data of the Alouette/ISIS database and ingests the Digisonde observations at the height of the maximum electron density and the TEC parameters calculated from GNSS receivers at the Digisonde locations to adjust the profiler with the real-time conditions of the ionosphere (Belehaki et al., 2012; Kutiev et al., 2012).

In summary the following groups of products are distributed from the DIAS user interface (<http://dias.space.noa.gr>): (1) real-time ionograms; (2) daily plots of critical frequencies and the Ionospheric Activity index over Europe; (3) now-casting and forecasting maps of ionospheric parameters (e.g., foF2, M(3000) F2, MUF); (4) nowcasting maps of the electron density up to the GNSS heights; (5) nowcasting maps of the TEC parameters; (6) alerts for forthcoming ionospheric disturbances in the European sector using data from the NASA/ACE mission. For the purposes of the project, DIAS products will be optimized to emphasize the effects of solar flares observed in the E and F ionospheric layers.

3. Development of new monitoring services and space weather prediction tools

3.1. Real-time optical imaging of the Sun

New image processing techniques and increased capacities of computing facilities make the production of high quality observations from Earth more feasible than ever. The development of real time data reduction and flare detection schemes based on H α imaging is relatively easy to implement in the computer facilities of an observing center (see e.g. Pötzi et al., 2015, and references therein).

In the PROTEAS project, it is planned that upon acquisition, solar H α images in fits format will be corrected for flat-field, dark current and limb darkening variation. Best frames will be selected as those least deformed by the atmospheric seeing, having the higher contrast. The fits header will contain all standard information (observation time, coordinates etc) along with a record of the reduction steps performed on the images (history). All reduction steps will be implemented through Interactive Data Language (IDL) routines, which are under development.

Since the imaging setup provides near full-disk images, the part of the solar disk where ARs are found may be constantly monitored. Additionally, a mosaic of images acquired once (at the beginning of the observations) or

twice per day will be created so that full-disk images will be provided as early in the day as possible. The aim is that the final products will be available shortly after the acquisition of images, for uploading on the HELIOSERVER (see Section 3.3).

3.2. Solar energetic particle events forecasting tool

The main objective is to develop a web-based tool capable of making forecasts of SEP events. The tool consists of two modules. The first module will target on the now-casting of the occurrence of SEPs and the second module will aim at the SEP flux profile including synoptic information on the peak intensity and duration.

For the prediction of SEPs, a novel reductive statistical scheme will be implemented. The statistical scheme was chosen on the basis of the operational functionality of the tool. Such, already available operational solutions are represented by but not limited to: the University of Málaga forecaster (UMASEP¹³), the Space Weather Prediction Center (SWPC¹⁴) forecaster at NOAA and, the most recent addition in this field, the Coronal Mass Ejection and Solar Energetic Particles (COMESep¹⁵) Alert system. Although, currently, several physics-based analytical models are in place to provide reliable interpretations on particle injection and SEPs accelerations (Aran et al., 2005), such efforts have not yet reached maturity and thus can not be used on an operational level. However, for more than three decades extensive statistical studies (Kahler et al., 2001; Garcia, 2004; Balch, 2008; Laurenza et al., 2009; Dierckxsens et al., 2015) have demonstrated the strong empirical relations that exist among SEPs and their parent solar sources paving the way for the implementation of forecasting operational tools. The basic input in such an approach is a well defined database of SEP characteristics (e.g. peak flux, fluence) and their parent solar events in terms of flare (magnitude, location) and CME (velocity, width); since the latter are made available in near-real time mode. Therefore, we have built such a new database, covering a large time-span, in an attempt to refine the basis of this forecasting effort.

Fig. 2 presents the preliminary output of the database. The SEP probability is defined as the quotient of the number of SEP events to the total number of events, in each of the six bins, while data on flare flux were retrieved by <ftp://ftp.ngdc.noaa.gov/STP/space-weather/solar-data/solar-features/solar-flares/x-rays/goes/>. Both panels present the SEP probability (y -axis) as a function of the flare flux (in W/m²; x -axis). Different lines correspond to different bins for the flare longitude ranging from -89 to 89 degrees. Evidently, when moving from east to west the probability for SEP occurrence increases. The basic difference among

¹³ Available at <http://spaceweather.uma.es/forecastpanel.htm>.

¹⁴ Available at <http://www.swpc.noaa.gov/content/wmo/solar-energetic-particles>.

¹⁵ Available at www.comesep.eu/alert.

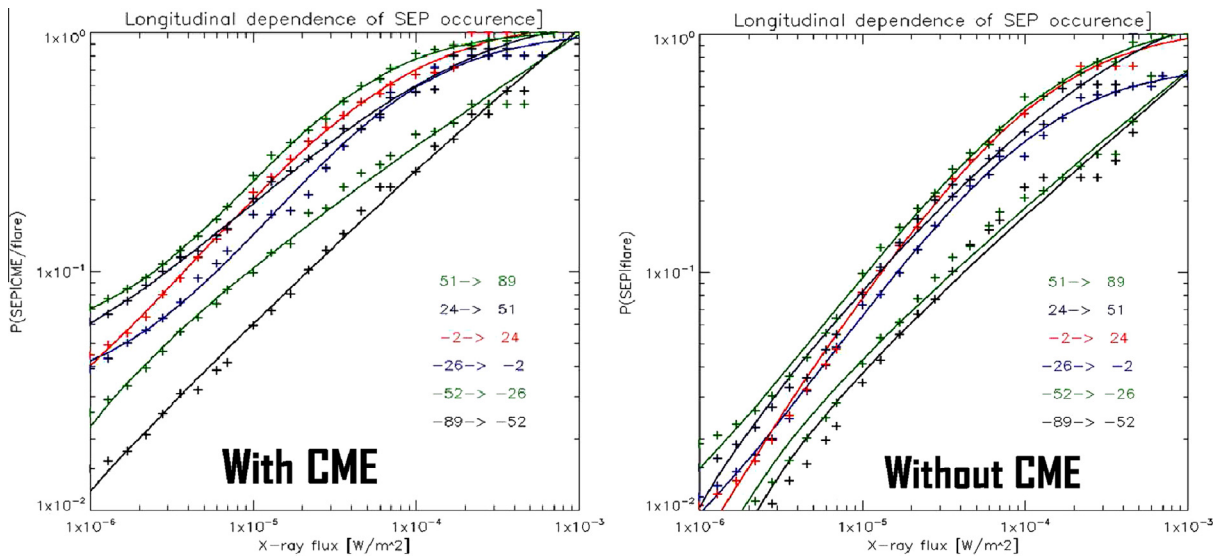


Fig. 2. SEP probability of occurrence as a function of GOES X-ray flux, for flares with (left panel) and without (right panel) CME. See text for details.

the two panels is the presence (or not) of a CME and clearly this factor is very important in terms of the SEP nowcasting. Virtually, all SEP events are accompanied by fast/broad CMEs and solar flares, which leads to the observational evidence that most likely both solar flares and CMEs are associated to SEP events constituting a new category of hybrid and/or mixed events (Kocharov and Torsti, 2002; Trotter et al., 2015). In terms of the SEP nowcasting, the information on the CME occurrence is used for the optimization of the binning for the local statistical model, which in turns reflects more accurately the expected probability of SEP occurrence. This is reflected in Fig. 2.

Since solar flare information is readily available in near-real time mode from various online solutions (i.e. Flaremail¹⁶, Solar DEMON¹⁷, SolarMonitor¹⁸, HEK¹⁹), the SEP prediction tool will utilize the information parched by one of these services, after a competitive evaluation. The basic input will be the location as well as the flux of the solar flare and the output will be the probability of SEP occurrence and the corresponding SEP characteristics as those defined here above. This shall be the first operational basis of the SEP prediction tool. With a view to an integrated forecasting system it is desirable that the SEP prediction scheme will utilize the output of a solar flare forecasting solution in order to retrieve the information on the flare and possibly CME occurrence, well before their

initiation, leading to a competitive advantage of the system.

3.3. HELIOSERVER and on-line provision

The HELIOSERVER, which is still under development, will contain a database with the output from the real time optical imaging of the Sun and the SEP prediction tool. This database will be available to the users of the on-line interface, providing the ability to search and request older H α images and SEP events. Since part of the project is to utilize the high quality data already available to the community, context data from space missions and links to their databases will also be provided through the HELIOSERVER. Thus data from space missions, such as the Solar Dynamics Observatory (SDO), the Geostationary Operational Environmental Satellites (GOES) and the ACE are planned to be included.

The SDO (Pesnell et al., 2012) was launched in February 2010 and since then it constantly monitors the solar atmosphere (corona and chromosphere) and the photospheric magnetic field. Two instruments are of particular interest to our task, the Atmospheric Imaging Assembly (AIA; Lemen et al., 2012) and the Helioseismic and Magnetic Imager (HMI; Schou et al., 2012). The former takes nearly simultaneous full disc images in ten wavelengths at visible, UV and EUV (from chromosphere to the corona) with 10 s cadence and 1 arcsec resolution. The latter produces full-disc continuous images, dopplergrams and magnetograms, both line-of-sight and vector.

GOES carries the Space Environment Monitor (SEM) which provides real-time data about the geospace environment.²⁰ The Energy Particle Sensor (EPS) provides the

¹⁶ A GOES X-ray flare detection alert, developed and operated at the Royal Observatory of Belgium (ROB), available at: <http://sidc.oma.be/products/flaremail/>.

¹⁷ The Solar Dimming and EUV wave Monitor (Solar DEMON), developed and operated at ROB, available at <http://solar demon.oma.be>, see also http://www.affects-fp7.eu/uploads/media/3_AFFECTS_User_WS_Kraaikamp_Solar_DEMON_Dimming_and_EUV_wave_Monitor_2013-02-28.pdf.

¹⁸ Available at: <http://www.solarmonitor.org/>, Gallagher et al., 2002

¹⁹ Heliophysics Events Knowledgebase, available at <http://www.lmsal.com/hek/>.

²⁰ See http://goes.gsfc.nasa.gov/text/GOES-N_Databook/databook.pdf for GOES-13 and later satellites.

incident flux density of alpha particles, protons and electrons over a range of energies. The X-ray Sensor (XRS) monitors the solar X-ray emission in the 0.5–4 Å and 1–8 Å bands with a temporal resolution of the average X-ray emission being 1 and 5 min. The emission level peak during a flare is used to determine its strength in a logarithmic scale (classes B,C,M,X). The Magnetic Field Sensor (MFS) is used to determine, in real-time, the magnitude and orientation of the magnetic field in the vicinity of the spacecraft.

Links to data from the ACE space mission will also be provided: The Magnetic Field Experiment (MAG; Smith et al., 1998) and the Electron, Proton and Alpha Monitor (EPAM; Gold and Krimigis, 1998) provide real time measurements on the magnetic field of the solar wind and its composition.

DIAS will be upgraded with additional sets, integrated in an interface with the HELIOSERVER and with improved techniques for the real-time quantification of the effects of solar eruptive events in the ionosphere. In this context, the HELIOSERVER will constitute a space weather facility and will be an extremely useful tool in advancing improvement of specific space weather services and supporting research. Integration of the data and observations from the monitoring services and the various space weather prediction tools will increase the existing capabilities. For instance, the following important ionospheric characteristics can be analyzed using this new space weather facility: (a) upon warning for a solar flare, the Athens Digisonde can set up a monitoring schedule for vertical ionograms at 2 s duration to detect immediate increase in the Ionospheric Electron Content (ITEC) and changes in the reflection height and (b) EUV and X-ray fluxes during flares can be used for postprocessing analysis of the effect in the ionospheric electron density measured by the Digisondes of DIAS and in the maps of the electron density

produced by the TaD model at different heights of the ionosphere.

4. Science cases

We demonstrate the expanded capabilities that the project may offer with two examples. The first one demon-

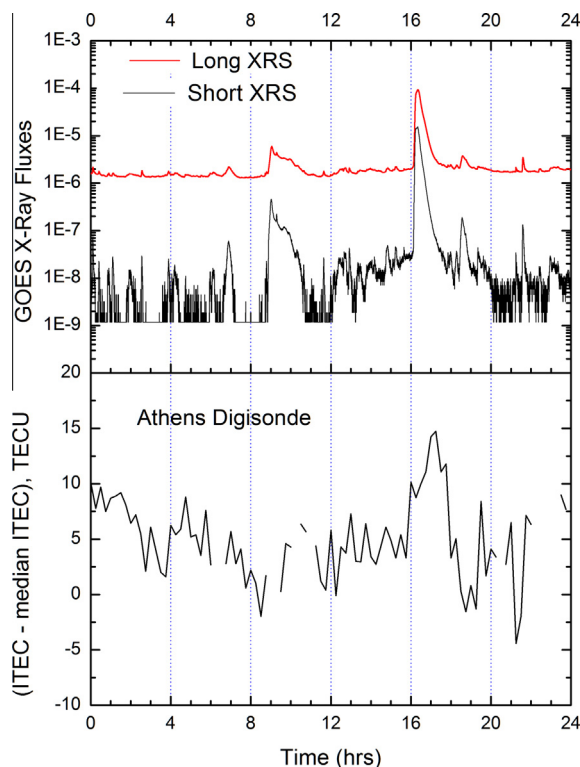


Fig. 4. Top: X-ray flux in the channels of GOES on July 8, 2014. The peak at ~16:20 UT is the M6.5 flare from AR12113. Bottom: the ionospheric TEC calculated by the Athens Digisonde manually scaled ionograms.

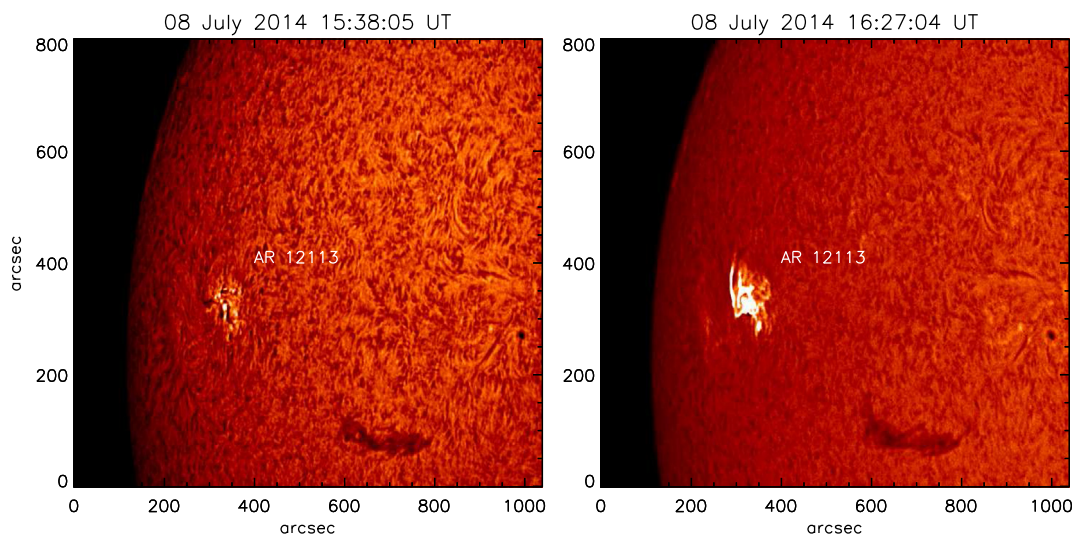


Fig. 3. H α close-up of the solar limb showing AR12113, before and during the flare. The images were taken with the setup described in Section 2.1.

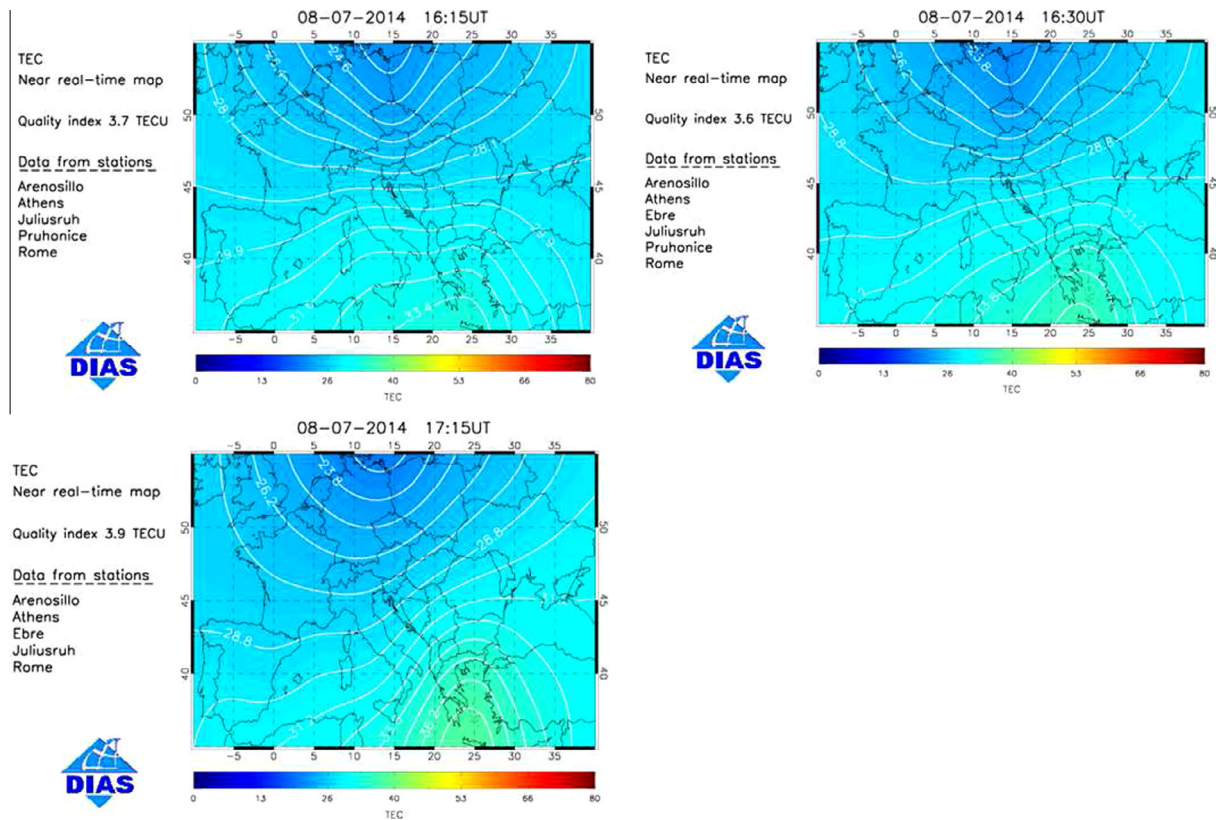


Fig. 5. The DIAS TEC nowcasting maps showing the evolution of the TEC disturbances over Europe on July 8, 2014 after the occurrence of the solar flare.

strates the effect on the ionosphere of a flare observed in H α incorporating chromospheric observations, X-ray fluxes and ionospheric conditions. The second example exploits the capabilities and effectiveness of the project components for a complete sequence of space weather events, from its initiation in the solar atmosphere (flare, CME, SEP event) to its impact on the interplanetary region (ICME) and ionosphere (flare, ICME, SEP event).

4.1. Solar flare effects on the ionosphere: Example of July 8, 2014

On July 8, 2014 a moderate solar flare from the AR12113 was observed by the solar telescope of NOA during its operational testing phase (Fig. 3). From the image sequences before and after the flare, the brightness excess of the AR in respect with the chromospheric background was calculated. It was found that near the peak time (Fig. 3, right panel) the average H α brightness of the AR had increased by a factor of three. Using a rough brightness threshold we estimated the flare area by counting the corresponding pixels whose brightness exceeded the threshold. The number of pixels was converted into area, after being corrected for projection effects. The area of a flare in H α may be used to categorize it in classes of “H α importance”, according to the nominal work of Švestka (1966). Thus, the (although roughly) estimated value of 178 micro-hemispheres is in agreement with the classifica-

tion of the flare as 1 N type, in the Kanzelhöhe Observatory database (<http://www.kso.ac.at>; Pötzi et al., 2015).

The GOES class of the flare was M6.5. In Fig. 4, X-ray fluxes recorded on this day (from NOAA/SWPC²¹) are presented, together with the ionospheric TEC data calculated by the Athens Digisonde manually scaled ionograms. Around 12:20 p.m. EDT (16:20 UTC), the SDO caught the explosion, which evolved into a CME that did not hit the Earth. The ITEC (bottom panel of Fig. 4) is the ionospheric part of the TEC calculated as the integral of the electron density from 90 km up to 700 km. ITEC shows a drastic increase that follows with a few minutes of delay the X-ray flux increase in GOES15. The increase in the electron density is also evident in the DIAS TEC maps that are generated through the implementation of the TaD model (Fig. 5). The first map at 16:15 UT corresponds to pre-flare conditions. The TEC increases at 16:30 UT, especially at lower latitudes, as the result of the flare. At 17:15 UT, the ionization starts to recover to pre-flare conditions.

4.2. SEP event prediction and its effects in the ionosphere

4.2.1. Background of the event

On March 7, 2012, an X5.4 flare (onset time: 00:02 UT; peak time: 00:24 UT; end time: 00:40 UT) at N17E27, was followed by an X1.3 flare (onset time: 01:05 UT; peak time:

²¹ <http://www.swpc.noaa.gov/products/goes-X-ray-flux>.

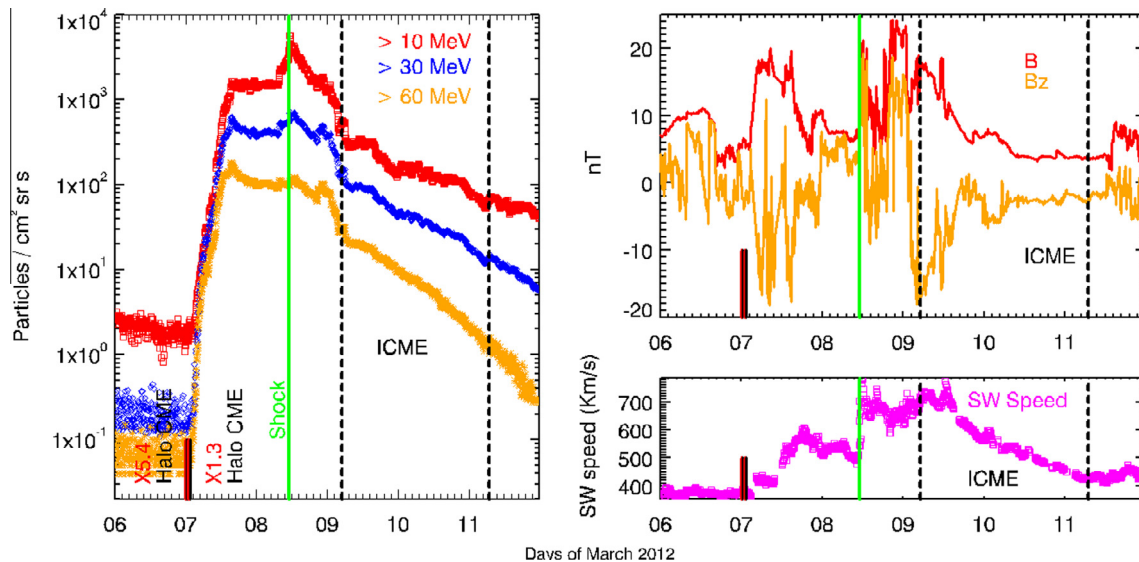


Fig. 6. The 7 March 2012 SEP event (left panel), the corresponding interplanetary magnetic field (IMF) data (top right panel) and the velocity of the solar wind (SW) (bottom right panel). Source: <http://omniweb.gsfc.nasa.gov/>; see text for details.

01:14 UT; end time: 01:23 UT) at N22E12. Two fast halo CMEs were reported by SOHO/LASCO, associated with these events. The first was observed above the occulting disk at 00:24 UT (with a speed of 2684 km/s), and the second at 01:30 UT (1825 km/s), respectively (Richardson et al., 2014). Fig. 6 (left panel), shows 5-min averaged integral GOES proton data at three energy ranges; namely, >10 MeV (red line); >30 MeV (blue line) and >60 MeV (orange line). The top panel on the right in Fig. 6 presents the IMF data. In particular the strength of the magnetic field B (in red) and its component B_z (in orange). The bottom panel on the right in Fig. 6, illustrates the solar wind (SW) speed. In all three panels, the following relevant information has been marked: the parent solar events (flares and CMEs) noted by short vertical lines, red for the solar flares and black for the associated CMEs; the green vertical line corresponds to the arrival of the shock at 1 AU, which identifies itself to the start time of a Sudden Storm Commencement (SSC). This is marked on March 8, 2012 at 11:03 UT. Furthermore, the start and end times of the corresponding ICME are noted with black dotted vertical lines. The ICME started on March 9, 2012 at 05:00 UT and lasted up until 11 March 2012 at 07:00 UT²².

4.2.2. Solar energetic particle event

On March 7, 2012, GOES satellites at $E_{mean} \sim 150$ MeV recorded an abrupt flux enhancement at around 2:20 UT. Velocity dispersion analysis (VDA) for the six GOES differential proton channels, ranging from $E_{mean} \sim 6$ to 150 MeV has been performed, in order to infer the corresponding solar release time (SRT) of the particles. As a result SRT was calculated to be $1:46 \pm 9$ min while the

path traveled by the particles was estimated to be 3.29 ± 0.20 AU. These results are consistent to the ones reported online by the SEPServer catalogues²³ (Vainio et al., 2013) that reported an SRT equal to $3:01 \pm 50$ min and a path of 3.84 ± 0.69 AU. The large inferred path traveled by the particles implies that those undergo significant scattering that resulted to delayed onset times at 1 AU. This is in line with the turbulent interplanetary space through which the particles traveled prior to their recording onboard different spacecraft, due to the intense solar events that preceded. Furthermore, since the time-profile of an SEP event strongly depends on the longitudinal location of the observer relative to its solar source, events associated to an eastern source are more gradual, with the CME-driven shock traveling a significant distance before intercepting IMF lines that are magnetically connected to the observer, which in turn leads to delayed onset times (Cane and Lario, 2006). This is also valid in the case of the March 07, 2012 SEP event since the parent solar flare was situated at N16E54. This event is a multi-spacecraft one and presented clear signatures in STEREO A (STA) and STEREO B (STB) spacecraft, in both protons and electrons (Papaioannou et al., 2014). Given the position of the spacecraft with respect to the source of the parent solar events, STB was best connected. The event's electron intensity at STB, was recorded at 1:15 UT (Papaioannou et al., 2014), while a clear increase was reported at $\sim 00:45$ UT (Richardson et al., 2014). Furthermore, high energy protons at STB presented an onset at 1:25 UT and the low energy ones at 2:40 UT. The reported timing of the particles is consistent with an association with the first flare-CME parent solar event and is inconsistent with

²² <http://www.srl.caltech.edu/ACE/ASC/DATA/level3/icmeTable2.htm>.

²³ <http://server.sepserver.eu/index.php?page=catalogue>.

an association with the second flare-CME parent solar event (Richardson et al., 2014). The SEP prediction tool yielded a probability of 68% for this SEP event which is rather high and thus corresponds to a successful nowcast issued by the system.

4.2.3. The ICME, the storm and the ionospheric disturbance

On March 9, 2012, a well pronounced ICME was marked at 1 AU (dotted black lines in all panels of Fig. 6). Given the relatively high SW speed and the negative IMF B_z component, that reached $-14.5 nT$ (see right panels of Fig. 6), a significant magnetic storm ($D_{st} = -148 nT$) occurred (Tsurutani et al., 2014). This magnetic storm was complex, since irregular characteristics were marked, especially in the extended and turbulent sheath region. This is most likely attributed either to the interaction of the successive fast halo CMEs in the interplanetary space; the presence of a coronal loop propagating outward of the Sun and the sweeping of coronal plasma by the outward propagating CME. In response to this ICME event, the DIAS system issued an alert for the occurrence of ionospheric storm time disturbances. The alert was issued on March 9, 2012 at 02:00 UT, giving a warning for the occurrence of positive storm effects in middle-to-low latitudes (up to 26% in respect to the normal

conditions) and the occurrence of negative storm effects in the middle-to-high latitude locations (up to 40% in respect to normal conditions) during the same day (<http://dias.space.noa.gr>). The predicted disturbances were successfully captured in the SWIF’s foF2 forecasts provided by DIAS. This is demonstrated in Fig. 7 together with the observed values and the monthly median estimates, which offer a measure of the ionospheric normal conditions, for two indicative locations: Chilton and Ebre in the higher and lower latitudinal zones, respectively. Besides the single site forecasts, the effects are also successfully captured by DIAS forecasting maps reflecting disturbances over the whole European region (Fig. 8). This example may be considered indicative of SWIF’s successful performance under enhanced geomagnetic activity related with geoeffective CME events (Tsagouri and Belehaki, 2015).

5. Summary and conclusions

We have presented one of the main objectives of the PROTEAS project, which will incorporate existing infrastructures and services of the IAASARS/NOA, as well as new monitoring services and promising prediction tools with a view of implementing a new space weather facility.

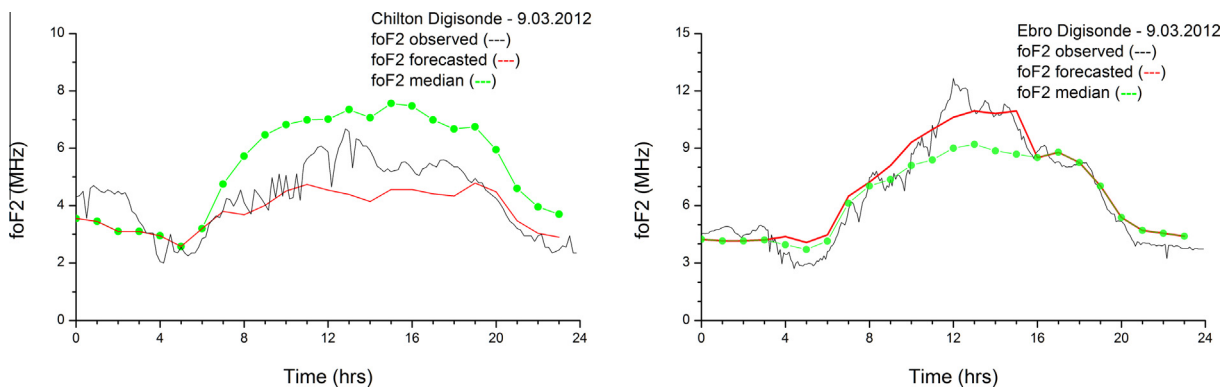


Fig. 7. CME effect in the ionization over Chilton and Ebre on March 9, 2012 (left and right respectively).

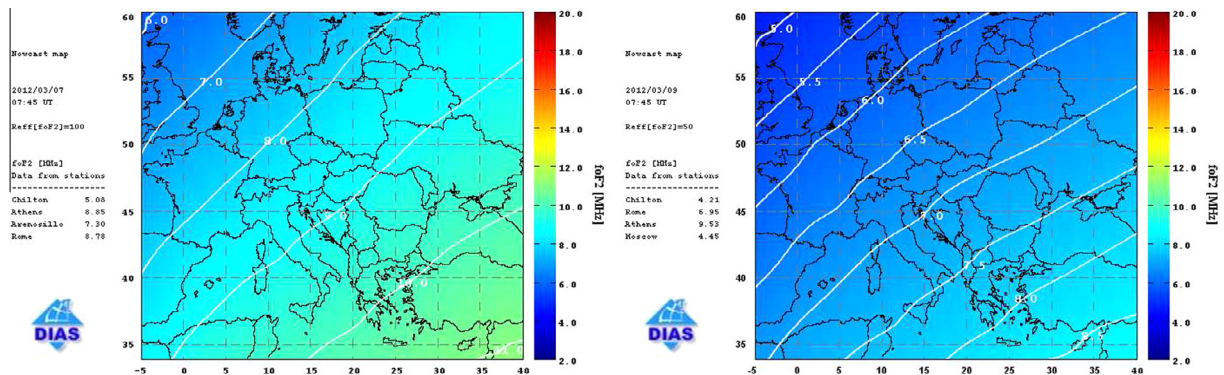


Fig. 8. foF2 maps from DIAS for March 7 and 9, 2012 (left and right respectively).

The project activities include the following monitoring and alerting/forecasting components.

- Chromospheric ground-based observations in H α along with real-time imaging in EUV from space will provide observations of flares and CMEs.
- Analysis of real-time ionograms from the Athens Digisonde to demonstrate potential local effects of solar flares over Athens. In addition daily plots of critical parameters such as I $T_{E}C$, foF 2 , hmE and hmF 2 can be updated in real-time to capture on-line possible flare effects in the structure of the ionosphere with height.
- The SEP prediction tool that will provide a SEP probability for each identified AR, according to its position and magnetic flux. In the case of a flare occurrence, this probability may be modified if associated with a CME.
- EUV, X-ray and particle fluxes obtained through open access space observatory data to follow flares and CMEs activity.
- Alerts for forthcoming ionospheric disturbances and maps of TEC and foF 2 parameters provided in real-time by DIAS are analyzed in combination with the data sets described above to get a full picture of ionospheric disturbances over Europe due to solar flares and CMEs.

Data, products and services will be openly available to the research community and operators of commercial and industrial systems through an on-line interface consisting of the products from the HELIOSERVER and DIAS, as well as links to the space observatories mentioned above. It should be emphasized that the key feature of the initiated project is the combination of the advanced DIAS capabilities, which are tuned to the monitoring of HF propagation conditions in the ionosphere, the NOAA's Digisonde that measures local ionospheric conditions, a co-located solar telescope and a SEP events prediction tool. The integration of these components will constitute a unique space weather facility in Greece.

One of the main characteristics of this new space weather facility, that distinguishes it from other projects, such as AFFECTS or COMESEP, relies on the exploitation of ground-based instruments and products, model results and tools already available or under development by the IAASARS/NOA researchers, as well as its potential to offer national and regional space weather services. In this sense, it is similar to the facility developed by the Bureau of Meteorology in Australia, which has the objective to provide a full range of space weather services focusing on the effects of solar flares in the ionosphere using observations from the network of Australian ground-based solar telescopes and ionosondes. Such regional warning centers exist in many countries around the globe and constitute a network operated by the International Space Environment Services (ISES²⁴) that offers important

services to a large number of users from various market sectors. The PROTEAS space weather center will be the first facility in Greece to operate with such specifications, offering the potential to evolve to a national, as well as regional, warning center for space weather. To this extent, PROTEAS forecasting products and services aim to address the needs of a wide range of users, including communication and space industry companies, civil security services and radio amateurs.

Another strategic advantage of this project is the ability to monitor the sequence of solar-terrestrial events through a wide range of instruments, spanning from their birth on the solar chromosphere to their effects down to the bottomside ionosphere. Bringing together data from different standing points is highly profitable for academic researchers, since the products of the PROTEAS project will be also available as raw data for analysis. Solar, space and ionospheric observations provided through this space weather center will offer the opportunity to test and improve the existing prediction schemes and the potential to develop new, more sophisticated methods of forecasting. The provided examples showcase this potential.

The good weather conditions in Athens are ideal for ground-based observations most days of the year and we believe that the H α observations, obtained by the solar telescope, will supplement the global network of full disk chromospheric observations from ground. H α imaging will allow the construction of a detailed solar flare database, containing chromospheric imaging and flare parameters, such as area and H α brightness, which are useful for their classification. An increasing statistical sample, will allow re-evaluations of the interconnection among chromospheric, X-ray emission and local ionospheric TEC that occur within minutes of a solar flare. On the other hand, simultaneous space measurements of particle fluxes, IMF magnetic field and the ionospheric parameter variations from the grid of the DIAS network along with SEP characteristics, resulting from flares and associated CMEs will allow a better insight on the solar-terrestrial connections in larger time-scales. Along with informing the users in near real-time, we believe that the components integrated into the space weather center of the PROTEAS project will also be an invaluable tool to investigate and showcase the details of such connections. This was highlighted by the science cases presented in Section 4 and we expect that it will bring added value to the project.

The existing ground-based facilities of IAASARS/NOA and the tools implemented by its academic staff (which provide unique datasets of chromospheric images, detailed ionospheric predictions and SEP probabilities), combined with publicly available data (provided by ongoing space missions) ensure the sustainability of the PROTEAS space weather center. We believe that its configuration also provides the potential of integrating, in the future, newly developed tools by IAASARS/NOA researchers.

²⁴ <http://www.ises-spaceweather.org/>.

Acknowledgments

The authors would like to thank the anonymous referees and the ASR guest editor Dr. Manolis Georgoulis for constructive comments that greatly improved the context of the manuscript. This work was performed in the framework of PROTEAS project within the KRIPIS action of the General Secretariat of Research and Technology, funded by Greece and the European Regional Development Fund of the European Union under the O.P. Competitiveness and Entrepreneurship, National Strategic Reference Framework (NSRF) 2007–2013 and the Regional Operational Program of Attica.

References

- Anastasiadis, A., 2002. Acceleration of solar energetic particles: the case of solar flares. *J. Atmos. Solar Terr. Phys.* 64, 481–488.
- Aran, A., Sanahuja, B., Lario, D., 2005. A first step towards proton flux forecasting. *Adv. Space Res.* 36, 2333–2338.
- Balch, C.C., 2008. Updated verification of the Space Weather Prediction Center's solar energetic particle prediction model. *Space Weather* 6, 1.
- Belehaki, A., Cander, Lj., Zolesi, B., et al., 2005. DIAS Project: The establishment of a European digital upper atmosphere server. *J. Atmos. Solar Terr. Phys.* 67, 1092–1099.
- Belehaki, A., Cander, Lj., Zolesi, B., et al., 2006. Monitoring and forecasting the ionosphere over Europe: The DIAS project. *Space Weather* 4, S12002.
- Belehaki, A., Cander, Lj., Zolesi, B., et al., 2007. Ionospheric specification and forecasting based on observations from European ionosondes participating in DIAS project. *Acta Geophys.* 55, 398–409.
- Belehaki, A., Tsagouri, I., Kutiev, I., et al., 2012. Upgrades to the Topside Sounders Model assisted by Digisonde (TaD) and its validation at the topside ionosphere. *J. Space Weather Space Clim.* 2, A20.
- Belehaki, A., Tsagouri, I., 2002. On the occurrence of storm-induced nighttime ionization enhancements at ionospheric middle latitudes. *J. Geophys. Res.* 107, 1209. <http://dx.doi.org/10.1029/2001JA005029>.
- Cane, H.V., Lario, D., 2006. An introduction to CMEs and energetic particles. *Space Sci. Rev.* 123, 45–56.
- Dierckx, M., Tziotziou, K., Dalla, S., et al., 2015. Relationship between solar energetic particles and properties of flares and CMEs: statistical analysis of solar cycle 23 events. *Solar Phys.* 290, 841–874.
- Fletcher, L., Dennis, B.R., Hudson, H.S., et al., 2011. An observational overview of solar flares. *Space Sci. Rev.* 159, 19–106.
- Gallager, P.T., Denker, C., Yurchyshyn, V., et al., 2002. Solar activity monitoring and forecasting capabilities at big bear solar observatory. *Ann. Geophys.* 20, 1105–1115.
- Gallagher, P.T., Moon, Y.-J., Wang, H., 2002. Active-region monitoring and flare forecasting—I. Data processing and first results. *Solar Phys.* 209, 171–183.
- Garcia, H.A., 2004. Forecasting methods for occurrence and magnitude of proton storms with solar soft X-rays. *Space Weather* 2, S06003.
- Gold, R.E., Krimigis, S.E., Hawkins III, D.K., et al., 1998. Electron, Proton, and Alpha Monitor on the Advanced Composition Explorer spacecraft. *Space Sci. Rev.* 86, 541–562.
- Jakowski, N.C., Mayer, C., Borries, C., Wilken, V., 2009. Space weather monitoring by ground and space based GNSS measurements. In: *Proc. ION – International Technical Meeting*, January 26–28, Anaheim, CA, 2009.
- Jakowski, N., Mayer, C., Hoque, M.M., Wilken, V., 2011. Total electron content models and their use in ionosphere monitoring. *Radio Sci.* 46, RS0D18. <http://dx.doi.org/10.1029/2010RS004620>.
- Kahler, S.W., Reames, D.V., Sheeley Jr., N.R., 2001. Coronal mass ejections associated with impulsive solar energetic particle events. *ApJ* 562, 558–565.
- Kocharov, L., Torsti, J., 2002. Hybrid solar energetic particle events observed on board SOHO. *Solar Phys.* 207, 149–157.
- Kutiev, I.P., Marinov, S., Fidanova, A., et al., 2012. Adjustments of the TaD electron density reconstruction model with GNSS TEC parameters for operational application purposes. *J. Space Weather Space Clim.* 2, A21.
- Laurenza, M., Cliver, E.W., Hewitt, J., et al., 2009. A technique for short-term warning of solar energetic particle events based on flare location, flare size, and evidence of particle escape. *Space Weather* 7, S04008.
- Lemen, J.R., Title, A.M., Akin, D.J., et al., 2012. The Atmospheric Imaging Assembly (AIA) on the Solar Dynamics Observatory (SDO). *Solar Phys.* 275, 17–40.
- Liu, J.Y., Lin, C.H., Tsai, H.F., Liou, Y.A., 2004. Ionospheric solar flare effects monitored by the ground-based GPS receivers: theory and observation. *J. Geophys. Res.* 109, A01307.
- Liu, H., Lhr, H., Watanabe, S., et al., 2007. Contrasting behavior of the thermosphere and ionosphere in response to the 28 October 2003 solar flare. *J. Geophys. Res.* 112, A07305.
- Papaioannou, A., Malandraki, O.E., Dresing, N., et al., 2014. SEPServer catalogues of solar energetic particle events at 1 AU based on STEREO recordings: 2007–2012. *A&A* 569, A96.
- Pesnell, W.D., Thompson, B.J., Chamberlin, P.C., 2012. The Solar Dynamics Observatory (SDO). *Solar Phys.* 275, 3–15.
- Pötzi, W., Veronig, A.M., Riegler, G., et al., 2015. Real-time flare detection in ground-based ha imaging at Kanzelhöhe Observatory. *Solar Phys.* 290, 951–977.
- Prössl, G.W., 1993. On explaining the local time variation of ionospheric storm effects. *Ann. Geophys.* 11, 1–9.
- Prössl, G.W., 1995. Ionospheric F-region storms. *Handbook of Atmospheric Electrodynamics*, vol. II. CRC Press, pp. 195–248.
- Richardson, I.G., von Rosenvinge, T.T., Cane, H.V., et al., 2014. 25 MeV proton events observed by the high energy telescopes on the STEREO A and B spacecraft and/or at earth during the first seven years of the STEREO mission. *Solar Phys.* 289, 3059–3107.
- Schou, J., Scherrer, P.H., Bush, R.I., et al., 2012. Design and ground calibration of the Helioseismic and Magnetic Imager (HMI) Instrument on the Solar Dynamics Observatory (SDO). *Solar Phys.* 275, 229–259.
- Smith, C.W., L'Heureux, J., Ness, N.F., et al., 1998. The ACE magnetic fields experiment. *Space Sci. Rev.* 86, 613–623.
- Švestka, Z., 1966. Optical observations of solar flares. *Space Sci. Rev.* 5, 388–418.
- Szuszczewicz, E.P., Lester, M., Wilkinson, P., et al., 1998. A comparative study of global ionospheric responses to intense magnetic storm conditions. *J. Geophys. Res.* 103, 11665–11684.
- Thomson, N.R., Rodger, C.J., Dowden, R.L., 2004. Ionosphere gives size of greatest solar flare. *Geophys. Res. Lett.* 31, L06803.
- Trottet, G., Samwel, S., Klein, K.-L., et al., 2015. Statistical evidence for contributions of flares and coronal mass ejections to major solar energetic particle events. *Solar Phys.* 290, 819–839.
- Tsagouri, I., 2011. Evaluation of the performance of DIAS ionospheric forecasting models. *J. Space Weather Space Clim.* 1, A02.
- Tsagouri, I., Belehaki, A., 2008. An upgrade of the solar-wind-driven empirical model for the middle latitude ionospheric storm-time response. *J. Atmos. Solar Terr. Phys.* 70, 2061–2076.
- Tsagouri, I., Belehaki, A., 2015. Ionospheric forecasts for the European region for space weather applications. *J. Space Weather Space Clim.* 5, A9. <http://dx.doi.org/10.1051/swsc/2015010>.
- Tsagouri, I., Belehaki, A., Moraitis, G., Mavromichalaki, H., 2000. Positive and negative ionospheric disturbances at middle latitudes during geomagnetic storms. *Geophys. Res. Lett.* 27, 3579–3582.
- Tsagouri, I., Koutroumbas, K., Belehaki, A., 2009. Ionospheric foF2 forecast over Europe based on an autoregressive modeling technique driven by solar wind parameters. *Radio Sci.* 44, RS0A35.
- Tsurutani, B.T., Verkhoglyadova, O.P., Mannucci, A.J., et al., 2009. A brief review of solar flare effects on the ionosphere. *Radio Sci.* 44, RS0A17.

- Tsurutani, B.T., Echer, E., Shibata, K., et al., 2014. The interplanetary causes of geomagnetic activity during the 7–17 March 2012 interval: a CAWSES II overview. *J. Space Weather Space Clim.* 4, A02.
- Tylka, A.J., Cohen, C.M.S., Dietrich, W.F., et al., 2005. Shock geometry, seed populations, and the origin of variable elemental composition at high energies in large gradual solar particle events. *ApJ* 625, 474–495.
- Vainio, R., Valtonen, E., Heber, B., et al., 2013. The first SEPServer event catalogue 68-MeV solar proton events observed at 1 AU in 1996–2010. *J. Space Weather Space Clim.* 3, A12.
- Webb, D.F., Howard, T.A., 2012. Coronal mass ejections: observations. *Living Rev. Sol. Phys.* 9, 1–83.
- Zolesi, B., Belhaki, A., Tsagouri, I., Cander, Lj.R., 2004. Real-time updating of the simplified ionospheric regional model for operational applications. *Radio Sci.* 39, RS2011.
- Zolesi, B., Cander, L.R., De Franceschi, G., 1993. Simplified ionospheric regional model for telecommunication applications. *Radio Sci.* 28, 603–612.